Materials Letters 280 (2020) 128562

Contents lists available at ScienceDirect

Materials Letters

journal homepage: www.elsevier.com/locate/mlblue

Synthesis and emission characteristics of lead-free novel Cs_4SnBr_6/SiO_2 nanocomposite

Vedi Santhana [a], Darius C. Greenidge [b], Dheivasigamani Thangaraju [a,*], R. Marnadu [c], T. Alshahrani [d], Mohd. Shkir [e]

[a] Nano-crystal Design and Application Lab (n-DAL), Department of Physics, PSG Institute of Technology and Applied Research, Coimbatore 641062, Tamil Nadu, India
[b] Shizuoka University, Office of the Special Advisor to the President, International Affairs (Geologist/Mineralogist), 836, Ohya, Suruga-ku, Shizuoka 422-8529, Japan
[c] Department of Physics, Sri Ramakrishna Mission Vidyalaya College of Arts and Science, Coimbatore 641 020, Tamil Nadu, India
[d] Department of Physics, College of Science, Princess Nourah Bint Abdulrahman University, Riyadh 11671, Saudi Arabia
[e] Advanced Functional Materials and Optoelectronics Laboratory (AFMOL), Department of Physics, College of Science, King Khalid University, Abha 61413, Saudi Arabia

ARTICLE INFO

Article history:
Received 3 July 2020
Received in revised form 4 August 2020
Accepted 18 August 2020
Available online 24 August 2020

Keywords:
Nanoparticles
Optical materials and properties
Nanocomposites
Luminescence

ABSTRACT

Lead-free Cs_4SnBr_6 nanostructures were synthesized using the high-temperature wet chemical method with as prepared cesium oleate and oleylammonium bromide. A new type of the SiO_2 layer formation method was followed using TEOS and m-cresol. Phase stability of the Cs_4SnBr_6 and Cs_4SnBr_6/SiO_2 aged samples was analyzed by the X-ray diffraction method. Transmission electron microscopy micrographs show that the hexagonally shaped particles covered with a thin SiO_2 layer for Cs_4SnBr_6/SiO_2 and were verified with TEM-EDS spectra. Synthesized particles showed a bright orange colour fluorescence emission under UV light and were confirmed with fluorescence emission spectroscopy.

1. Introduction

Organic and all-inorganic halide perovskites have fascinated the devotion of scientist due to their rich optical and electrical properties such as high carrier mobility, tunable direct bandgap, high absorption, and low existing banding energy [1–4]. Cs_nXY_{2+n} (X = Pb, and Sn; Y = Cl, Br, and I) are the possible combinations of lead-free halide perovskites $CsXY_3$, Cs_2XY_4 and Cs_4XY_6. $CsXY_3$ and Cs_2XY_4 combinations were widely researched and its emission was reported. Recently, research results of Cs_4XY_6 compound is still a mystery and researchers concentrate on different synthesis conditions and emission strategy. Green emission of Cs_4PbBr_6 is upon the synthetic conditions due to energy transfer between Pb^{2+} ions and green emission centers, intrinsic defects within its wide bandgap. Origin of emission from Cs_4PbBr_6 is still debated, and still the research is in progress to understand the emission. Cs_4PbBr_6 shows narrow excitonic photoluminescence at only low temperature and wavelengths <400 nm. In the case of Cs_4SnBr_6 exhibits broad band green yellow PL spectra at room temperature.

The lead-based halide perovskites are capable of many real-time usages like solar cells, photocatalytic, lasers, LEDs, solar cells, single photon sources, photodetectors, and sensor applications. Even though it is a material of high potential, the disadvantages of toxic lead elements restrict commercialization [5–7]. The Goldschmidt's tolerance factor (t) for structure of perovskites:

$$t = \frac{(R_A + R_B)}{\sqrt{2}(R_B + R_X)}$$

here R_A, R_B, and R_x are ionic radii of A, B, and X, and when t is ranged between 0.75 and 1.0, the structure of perovskite could be predicted. Lead free elements like Sn, Bi, In, and Sb are the suitable alternatives for the Pb site. Among them, Sn found to be best replacement nontoxic material that has the same characteristic behavior of Pb, according to the t factor of Goldschmidt [8–10]. The transition metal cations and Sn^{2+}, are the effective replacements for Pb^{2+},which was advantageous for direct bandgap semiconductors [11]. The Sn-based compounds have higher luminescence efficiency and carrier mobility than Pb based halide perovskite. Perovskites based on Sn(II) are vulnerable to oxidation, which can generate defects with high density in lattices, generally consequential in their low PLQYs.

Phase stability of all-inorganic lead-free halide perovskite can be achieved with suitable surface modification such as with a non-halide ceramic material or biocompatible layer coating. SiO_2, TiO_2, and CdS layer capped halide perovskites gave rise to the

* Corresponding author. Tel: +91 8098768306.
E-mail address: thangaraju@psgitech.ac.in (D. Thangaraju).

https://doi.org/10.1016/j.matlet.2020.128562
0167-577X/

production of a layer to control degradation of these materials due to normal ambient conditions. New external layer growth on unstable lead-free halide perovskite is still a challenging process due to inconsistent temperature and growth conditions. Available methods of composite halide perovskite are suitable only for a particular type of halide perovskite, not for all kinds.

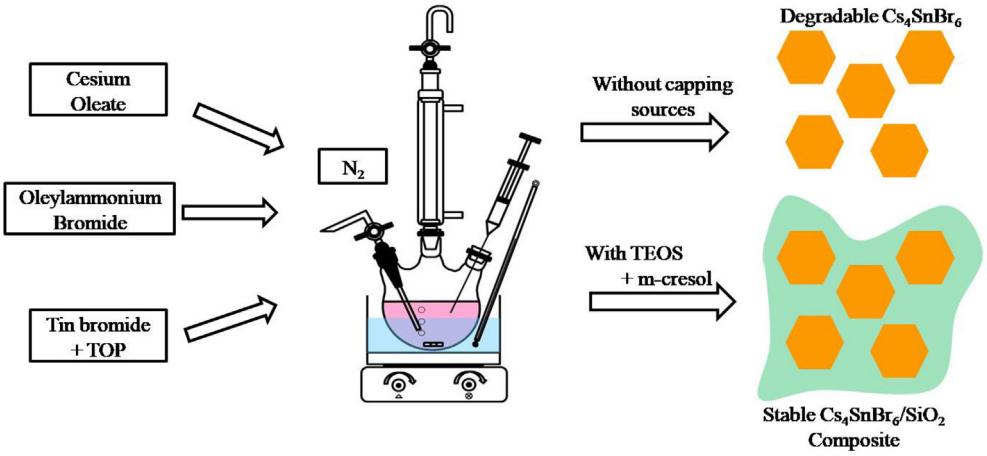

Fig. 1. Schematic diagram of synthesis of Cs_4SnBr_6/SiO_2.

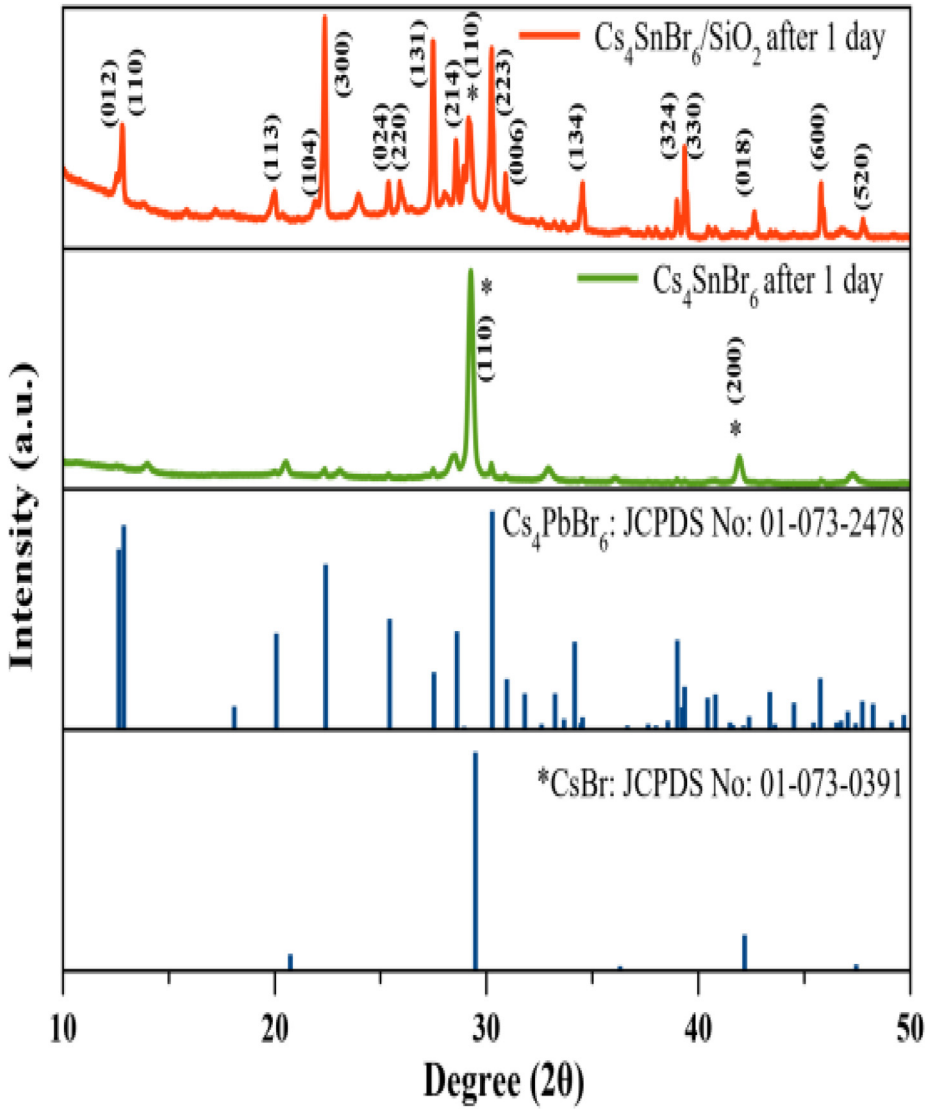

Fig. 2. Comparative XRD patterns of Cs_4SnBr_6 and Cs_4SnBr_6/SiO_2 nanostructures.

In this work, lead-free Cs_4SnBr_6 with a mild layer of SiO_2 composite was constructed using a two-step hot injection synthesis method. Phase stability, morphology, and luminescence measurements of synthesized composite Cs_4SnBr_6/SiO_2 were analyzed.

2. Experimental methods

The two-step hot injection method was used to prepare Cs_4SnBr_6 nanocubes using pre-synthesized cesium oleate (Cs-OA) and oleyl-ammonium bromide (OLA-Br). For the synthesis of Cs-OA synthesis, cesium carbonate (1.62 g, Cs_2CO_3) along with oleic acid, and 1-Octadecene (1:4) were loaded into 100 ml three-neck flask. The temperature of the mixture was degassed at 110 °C and was further kept at 150 °C under N_2 atmosphere for 1 h. In a separate flask, the desired volume of hydrogen bromide (HBr) was loaded with oleylamine into a three-neck flask for the preparation of the OLA-Br stock solution. The above solution was degassed at 110 °C and was further heated at 150 °C under N_2 atmosphere. The solution was collected and stored at the N_2 filled screw-type septa. In a typical combination, tin (II) bromide (SnBr) was added with 2 ml of tri n-octylphosphine (TOP) in 100 ml three-neck flask, and the solution was degassed for 20 min at 120 °C. The preheated OLA-Br was injected to above degassed solution under N_2 atmosphere. Then the solution temperature was raised to 160 °C, and 2 ml of Cs-OA was then injected into the three-neck flask. The final solution was stirred for 5 min and quenched to room temperature. The cooled solution was washed with hexane for further use. In a typical synthesis of Cs_4SnBr_6/SiO_2 capping, the same procedure was followed as the Cs_4SnBr_6 preparation until the cesium oleate injection. After injection of cesium oleate, the solution was allowed to cool down to 80 °C; 2 ml TEOS and 250 μl of m-cresol were injected for the formation of SiO_2 layer. The centrifuging of crude solution at 4500 rpm for 5 min was done and dispersed in hexane. Schematic diagram of synthesis of Cs_4SnBr_6/SiO_2 was presented in Fig. 1.

3. Results and discussion

The XRD profiles were logged for Cs_4SnBr_6 and Cs_4SnBr_6/SiO_2 with a scan rate of 3°/min angle range between 10 and 50° using Empyrean, Malvern Panalytical instrument equipped with CuK_α (λ = 1.54 Å). Acquired XRD patterns of Cs_4SnBr_6 and Cs_4SnBr_6/SiO_2 were analyzed after 24 h of synthesis to check its stability. The results are shown in Fig. 2. The pattern for Cs_4SnBr_6 revealed that there are two types of particles present in the sample. Low intensity peaks were matched with Cs_4SnBr_6 (Cs_4PbBr_6, JCPDS # 01-073-2478) along with CsBr (JCPDS # 01-073-0391). The observed XRD pattern for Cs_4SnBr_6/SiO_2, having a rhombohedral structure, matched well with the similar structure for Cs_4PbBr_6 (JCPDS # 01-073-2478). XRD of previously reported results for Cs_4SnBr_6, also matched well with the present results [12,13]. From the XRD analysis, it was observed that SiO_2 capping of Cs_4SnBr_6, having higher stability than as-synthesized Cs_4SnBr_6, was present under ambient conditions. The XRD data derived for Cs_4SnBr_6 and Cs_4SnBr_6/SiO_2 samples after 2 days indicates that complete

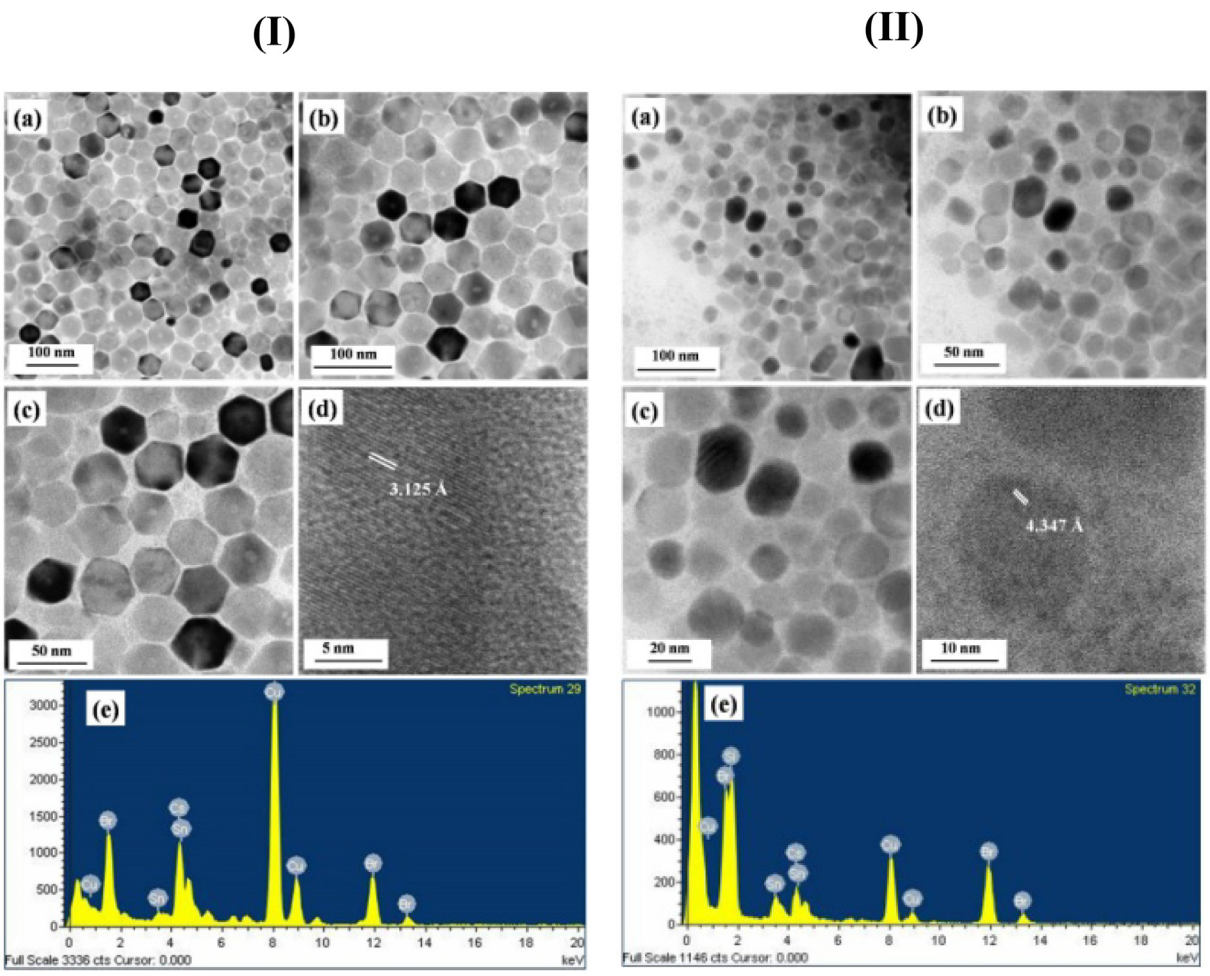

Fig. 3. TEM (a, b, and c), HRTEM (d) and EDX (e) images of (I) Cs_4SnBr_6 and(II) Cs_4SnBr_6/SiO_2 composite nanostructures.

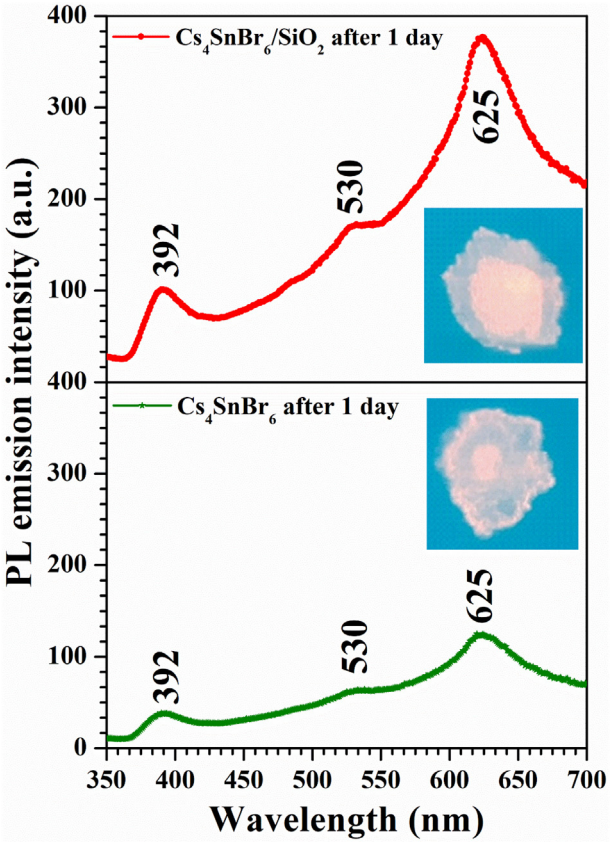

Fig. 4. Fluorescence spectra of Cs_4SnBr_6, Cs_4SnBr_6/SiO_2 and real time emission (inset).

decomposition was occurred for both samples (Fig. S1) (see supplementary data file).

The particle morphology of as-synthesized Cs_4SnBr_6 and Cs_4SnBr_6/SiO_2 were analyzed using a JEOL TEM 2100F and captured TEM/HRTEM images are shown in Fig. 3(I) and (II). The observed morphology for Cs_4SnBr_6 is a monodispersed honeycomb with ~25 nm size (Fig. 3(I)). HRTEM images show that an inter-planner distance of 4.125 Å belongs to the (1 1 0) plane of CsBr, which is evidence that the particles were degraded under ambient conditions. Tin presence in EDX spectra revealed that the Cs_4SnBr_6 material is not fully degraded. In Fig. 3(II), TEM images confirmed that the particles of Cs_4SnBr_6 were covered with a thin layer of amorphous SiO_2. Lattice images show an inter-planner distance of 4.347 Å, which is the (1 1 3) plane of Cs_4PbBr_6, which has a similar structure to that of Cs_4SnBr_6. The EDX of the respective particles revealed the presence of Si in the system, which covers as a thin layer of SiO_2 over the Cs_4SnBr_6 particles.

Luminescence spectroscopy of Cs_4SnBr_6 and Cs_4SnBr_6/SiO_2 particles were analyzed using an Agilent Fluorescence Spectrometer, with ranges between 300 and 700 nm under 340 nm excitation (Fig. 4). The samples were analyzed after 24 h of synthesis, in which Cs_4SnBr_6 shows three less intense peaks at 392, 530, and 625 nm. High intensity 392, 530, and 625 nm emissions were observed for the Cs_4SnBr_6/SiO_2 composite, which revealed the greater emission stability of the SiO_2 capped Cs_4SnBr_6 than that of bare Cs_4SnBr_6 samples. Previous reports on Cs_4SnBr_6 showed green (530 nm) as well as bright orange (625 nm) emissions. Just as for Cs_4PbBr_6, the Cs_4SnBr_6 structure is also composed of $[SnBr_6]^{4-}$ octahedra separated by Cs^+ ions [14,15]. Defects which originated from the vacancy of Br, or the inclusion of –OH, can be the reason for the orange emission (625 nm) from Cs_4SnBr_6, which exhibits the similar emission property of Cs_4PbBr_6 and at the same time 530 nm emission raised from self-trapped exciton (STE) of Cs_4SnBr_6. Normalized emission spectrum comparison of Cs_4SnBr_6 and Cs_4SnBr_6/SiO_2 was given in supplementary data Fig. S2(see supplementary data file). Emission arrived at 392 nm is originated from CsBr presents in both samples. The blue emission was STE luminescence of CsBr, which is well established from previous results [16].

4. Conclusion

Lead-free facile Cs_4SnBr_6 and Cs_4SnBr_6/SiO_2 were successfully synthesized by the two-step hot injection method using high boiling point solvent. The SiO_2 capping for the Cs_4SnBr_6/SiO_2 composite was also a success that arrived at by using TEOS and m-cresol at 80 °C. The XRD peaks were evidence that the synthesized particles were of highly crystalline nature, which was confirmed using TEM/HRTEM. EDX revealed that a SiO_2 layer covered the Cs_4SnBr_6. Luminescence spectroscopy showed that the synthesized Cs_4SnBr_6 and Cs_4SnBr_6/SiO_2 particles emit a fluorescence of bright orange colour.

Declaration of Competing Interest

The authors declare that they have no known competing financial interests or personal relationships that could have appeared to influence the work reported in this paper.

Acknowledgement

The Author (D. Thangaraju) sincerely thanks SERB (ECR/2017/002974), DST, India, for the financial support. T Alshahrani is thankful to Deanship of Scientific Research at Princess Nourah bint Abdulrahman University for funding this work through the Fast-track Research Funding Program.

Appendix A. Supplementary data

Supplementary data to this article can be found online at https://doi.org/10.1016/j.matlet.2020.128562.

References

[1] X. Li, F. Cao, D. Yu, et al., Small 13 (2017) 1603996.
[2] G. Pan, X. Bai, D. Yang, et al., Nano Lett. 17 (2017) 8005.
[3] W. Xu, X. Chen, H. Song, Nano Today 17 (2017) 54–78.
[4] H. Siddiqui, Mater. Lett. 249 (2019) 99–103.
[5] D. Li, W. Xu, D. Zhou, et al., J. Lumin. 216 (2019) 116711.
[6] Y.H. He, M.M. Liu, N. Darabedian, et al., Inorg. Chem. 53 (2014) 2822.
[7] L.J. Lawton, W.E. Donaldson, Biol. Trace Elem. Res. 28 (1991) 83.
[8] P. Gao, M. Gratzel, M.K. Nazeeruddin, Energy Environ. Sci. 7 (2014) 448.
[9] S. Chatterjee, A.J. Pal, J. Mater. Chem. A 6 (2018) 3793.
[10] A. Babayigit, A. Ethirajan, M. Muller, B. Conings, Nat. Mater. 1 (2016) 247.
[11] X. Wang, T. Zhang, Y. Lous, Y. Zhao, Mater. Chem. Front. 3 (2019) 365.
[12] R. Chiara, Y.O. Ciftci, V.I.E. Queloz, M.K. Nazeeruddin, G. Grancini, L. Malavasi, J. Phys. Chem. Lett. 11 (2020) 618.
[13] L. Tan, W. Wang, Q. Li, et al., Chem. Commun. 56 (2020) 387.
[14] J. Yin, Y. Zhang, A. Bruno, C. Soci, O.M. Bakr, J.L. Bredas, O.F. Mohammed, ACS Energy Lett. 2 (2017) 2805.
[15] B.M. Benin, D.N. Dirin, V. Morad, M. Wçrle, S. Yakunin, G. Rainm, O. Nazarenko, M. Fischer, I. Infante, M.V. Kovalenko, Angew. Chem. Int. Ed. 57 (2018) 11329.
[16] G.A. Appleby, J. Zimmermann, S. Hesse, H. von Seggern, J. Appl. Phys. 109 (2011) 013507.